Malaysian Applied Biology
https://doi.org/10.55230/mabjournal.v54i3.3010

Research Article

Differentially Expressed Proteins in *Corynebacterium pseudotuberculosis* During Biofilm Formation

Anati Abd Rashid Syaida[1], Faez Firdaus Abdullah Jesse[2], Mohd Shafiq Aazmi[1], Mohd Izwan Mohamad Yusof[1], Mohd Fakharul Zaman Raja Yahya[1,3]*

1. Faculty of Applied Sciences, Universiti Teknologi MARA, 40450 Shah Alam, Selangor, Malaysia
2. Faculty of Veterinary Medicine, Universiti Putra Malaysia, 43400 UPM Serdang, Selangor, Malaysia
3. Integrative Pharmacogenomics Institute (iPROMISE), Universiti Teknologi MARA, Bandar Puncak Alam 42300, Shah Alam, Selangor, Malaysia

*Corresponding author: fakharulzaman@uitm.edu.my

ABSTRACT

Corynebacterium pseudotuberculosis is a non-motile, β-hemolytic bacterium and causative factor of caseous lymphadenitis. The disease affects sheep and goats, causing impaired wool production, weight loss, and carcass condemnation. Our previous work has elucidated the morphology, heterogeneity, and antimicrobial susceptibility of *C. pseudotuberculosis* biofilm. However, the information on proteome expression underlying *C. pseudotuberculosis* biofilm development remains scarce. Thus, the objective of the present work is to compare the whole-cell proteome profiles between planktonic and biofilm fractions of *C. pseudotuberculosis* and identify *C. pseudotuberculosis* proteins and biological pathways showing differential expression. *C. pseudotuberculosis* biofilm was grown in a six-well microplate for 24 hr at 37°C. Polyacrylamide gel electrophoresis combined with tandem mass spectrometry and bioinformatics analysis was conducted to analyze proteome expression. Results demonstrated differential expression of seven SDS-PAGE protein bands (33.7 – 150 kDa) in comparison between the planktonic and biofilm fractions of *C. pseudotuberculosis.* Overall, 711 proteins that showed differential expression were successfully identified, while the protein-protein interaction network revealed a total of 3868 functional linkages among the differentially expressed proteins. Fifty-seven hub proteins with more than 10 functional linkages were identified, including large subunit ribosomal protein L3, translation initiation factor IF-2, multifunctional oxoglutarate decarboxylase, and DNA-dependent RNA polymerase. Functional enrichment analysis revealed the association of differentially expressed *C. pseudotuberculosis* proteins with secondary metabolite metabolism (*p-value*<0.05). In conclusion, differential protein expressions in *C. pseudotuberculosis* may modulate adaptive responses to environmental stressors, thereby promoting biofilm formation.

Key words: Biofilm, caseous lymphadenitis, *Corynebacterium pseudotuberculosis*, proteomics

INTRODUCTION

Corynebacterium pseudotuberculosis, a Gram-positive bacterium, belongs to the Actinomycota order (Gomide *et al*., 2018; Eberle *et al*., 2018). It is also a β-hemolytic and non-motile pathogen causing caseous lymphadenitis (CLA). CLA or cheesy gland in sheep and goats caused by this animal pathogen often contributes to significant economic losses and is frequently observed across sheep-rearing countries globally, such as Australia, New Zealand, South Africa, the United States, Canada, Brazil, Iran, Egypt, and Malaysia (Soares *et al*., 2013). Common consequences of CLA are low milk production, reduction in body weight, and death (Eberle *et al*., 2018).

In the last few years, the studies of proteome expression in biofilm-forming pathogens have dramatically increased (Othman & Yahya, 2019; Zawawi *et al*., 2020; Cho *et al*., 2024; Sung *et al*., 2025). This is because proteins are well understood to play major roles in biofilm formation, a microbial survival strategy that allows microorganisms to form a stable community in a dynamic environment. They initiate bacterial adhesion to the surface, provide mechanical stability, and form a cohesive network to support the biofilm cells. Investigating the proteome composition of both planktonic and biofilm states of a microbe is essential for understanding the molecular mechanisms underlying their phenotypic and functional differences, which have critical implications for microbial pathogenicity, antibiotic resistance, and industrial applications (Dsouza *et al*., 2024). Biofilms exhibit distinct proteomic profiles compared to their planktonic counterparts due to altered gene expression and metabolic pathways that confer enhanced resilience, adhesion, and extracellular matrix production (Stoodley *et al*., 2002; Percival *et al*., 2015; Sung *et al*., 2024), making them notoriously resistant to antimicrobial treatments. By characterizing these proteomic variations, researchers can identify key proteins and pathways involved in biofilm formation, maintenance, and dispersal, which may serve as potential targets for novel therapeutic strategies or biofilm inhibition in medical settings.

Previous works have characterized *C. pseudotuberculosis* biofilm in terms of structure, biochemical composition, and antimicrobial susceptibility (Yaacob *et al*., 2021a; Rashid *et al*., 2022); however, the study related to the proteomic changes

Article History
Accepted: 4 August 2025
First version online: 30 September 2025
Cite This Article:
Syaida, A.A.R., Jesse, F.F.A., Aazmi, M.S., Yusof, M.I.M. & Yahya, M.F.Z.R. 2025. Differentially expressed proteins in *Corynebacterium pseudotuberculosis* during biofilm formation. Malaysian Applied Biology, 54(3): 15-26. https://doi.org/10.55230/mabjournal.v54i3.3010

during *C. pseudotuberculosis* biofilm development is still scarce. Thus, the objective of this work was to compare the whole-cell proteome profiles between planktonic and biofilm fractions of *C. pseudotuberculosis* and identify *C. pseudotuberculosis* proteins and biological pathways showing differential expression. The present study used a combination of subtractive proteomic and protein-protein interaction network analyses (Yahya *et al*., 2017) to decipher the differential proteomic expression in *C. pseudotuberculosis* biofilm and to elucidate the unexplored functional links in understanding this veterinary pathogen.

MATERIALS AND METHODS

Test microorganism

A clinical isolate of *C. pseudotuberculosis* was provided by the Veterinary Laboratory Service Unit at Universiti Putra Malaysia (UPM). The microorganism was maintained in nutrient broth at 37°C overnight to achieve the optical density OD 600 = 0.5 for the biofilm formation assay.

Biofilm formation assay for FESEM and proteomics analyses

C. pseudotuberculosis biofilm was grown on a sterile glass cover slip in a six-well microplate (Yaacob *et al*.,2021). Bacterial inoculum (4 mL) and fresh nutrient broth (1 mL) were loaded into the microplate wells. After 24 hr incubation at 37°C, the glass cover slip was removed and rinsed with saline buffer twice. For the proteomics experiment, the same microplate protocol was performed without the sterile glass cover slip.

FESEM analysis

The biofilm structure of *C. pseudotuberculosis* was studied using FESEM (Hitachi, Japan) (Yaacob *et al*.,2021). After fixation in 4% (v/v) formaldehyde for 3 hr, the biofilm on the glass cover slip was rinsed with sterile distilled water thrice, dehydrated using absolute ethanol for 10 min, and air dried overnight. Observation was performed at 5,000x magnification.

Extraction and determination of whole-cell proteins

After 24 hr incubation, the nutrient medium was transferred to a microcentrifuge tube, while the biofilm fraction was rinsed with 0.9% (w/v) NaCl twice and scraped from the surface before being transferred to another microcentrifuge tube (Yahya *et al*., 2017). Both planktonic and biofilm fractions were analyzed for whole-cell proteome expression. They were pelleted at 10,000 rpm for 10 min. Then, they were incubated in a lysis buffer containing 1 mM PMSF and 0.5% (w/v) SDS at 95°C for 15 min and centrifuged at 10,000 rpm. The standard Bradford assay was performed to determine protein concentration.

1D-SDS-PAGE analysis

The protein samples were separated by 1D-SDS PAGE (Yahya *et al*., 2017). 1X SDS sample buffer was used to solubilize the protein samples and heated at 95°C for 5 min. 12 % (v/v) polyacrylamide gel was used to separate protein samples and protein standards (10-245 kDa) for 50 min at 200 V. Gel staining was performed using G250 Coomassie-Blue and analyzed using ImageJ software. All protein bands were digested using trypsin and identified using LC-MS/MS.

Trypsin digestion

The selected protein bands were incubated in acetonitrile: distilled water (50:50) containing 25 mM ammonium bicarbonate for 45 min, vacuum-dried, and stored at -20°C (Yahya *et al*., 2017). Each of the gel slices was then treated with 10 µL of 12.5 µg/mL trypsin with 25 mM ammonium bicarbonate at 37°C overnight. The digested peptides were incubated in 10 mL of acetonitrile containing 1% (v/v) trifluoroacetic acid for 20 min, vacuum-dried, and desalted. The concentration of eluted peptide was measured using the NanoDrop spectrophotometer.

LC-MS/MS analysis

LC-MS/MS was used to determine the identity of *C. pseudotuberculosis* proteins. The tryptic peptides were analyzed using HPLC combined with a TripleTOF mass spectrometer (AB SCIEX, USA) (Yahya *et al*., 2017). The parameter settings in the mass spectrometer were as follows: Interface heater temperature (IHT) of 150°C, ion spray voltage floating (ISVF) of 2300 V, and declustering potential (DP) of 70 V. A MS survey scan (350 – 1250) and MS/MS scan (100 & 1800) were used herein. Mass spectra were analysed using the Mascot search engine (Matrix Science) and the SwissProt database. The search parameters used were as follows: i) mass values: monoisotopic; ii) peptide mass tolerance: ±0.2 Da; iii) miss cleavage: 1; iv) variable modifications: phospho (ST), phospho (Y). Proteins with two or more peptides were chosen for high-confidence protein identification.

Phosphoprotein analysis

ProQ diamond assay was performed to validate biofilm phosphoproteins identified in the LC-MS/MS analysis (Yahya *et al*., 2017). The gels were treated using 10% (v/v) trichloroacetic acid, 50% (v/v) methanol for 30 min at 60 rpm, rinsed with ultrapure water for 10 min, and incubated in the fluorescent dye in the dark for 60 min at 60 rpm. The gels were destained using 50 mM sodium acetate, 20% (v/v) acetonitrile, pH 4.0, in the dark for 30 min at 60 rpm. A gel documentation system (Alpha Innotech, CA) was used to visualize and photograph fluorescently labelled phosphoproteins.

Analysis of functional classification

Classification of protein function was performed by SwissProt/TrEMBL database search. All identified proteins were classified according to their functional categories and subcellular localizations.

Analysis of the functional network of interactive proteins

The identified *C. pseudotuberculosis* proteins were used as queries in the STRING database v.11.0 to construct the high-confidence network of protein linkages.

Analysis of a hypothetical protein

The selected hypothetical protein was analyzed for transmembrane helices, functional domains, post-translational modification sites, physicochemical properties, 3D structure, and functional linkages using TMHMM 2.0, SMART ScanProsite, ProtParam, SWISS-MODEL, and STRING database, respectively.

RESULTS

Heterogeneous biofilm formed by *C. pseudotuberculosis*

It was clear that *C. pseudotuberculosis* formed a heterogeneous three-dimensional biofilm structure (Figure 1). The biofilm cells were surrounded by extracellular matrix.

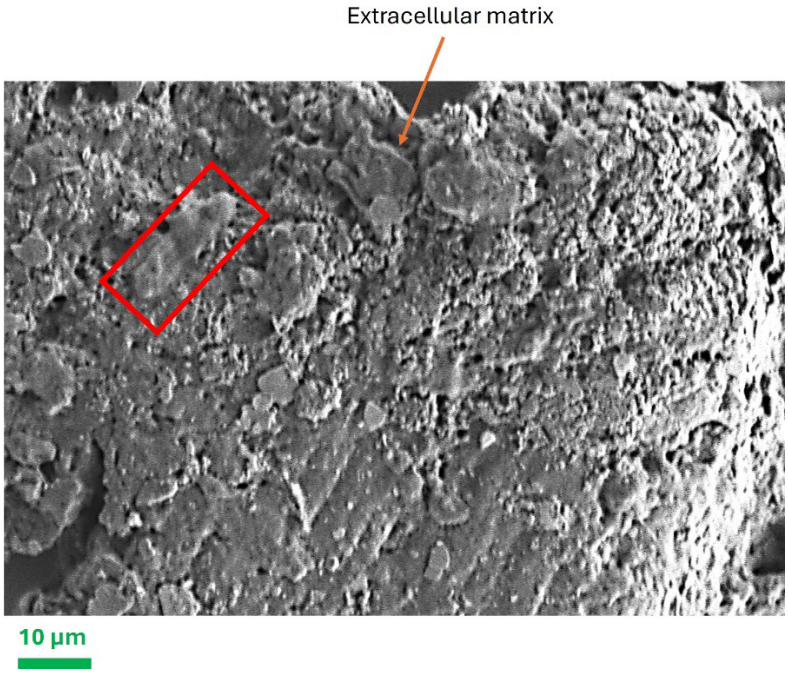

Fig. 1. FESEM image of heterogeneous biofilm of *C. pseudotuberculosis* at 5000x magnification. Red box: biofilm cell.

Whole-cell proteome profiles

Both planktonic and biofilm fractions shared the same nine protein bands, namely 33.7 kDa, 41.9 kDa, 50 kDa, 58.5 kDa, 67 kDa, 75 kDa, 100 kDa, 128.8 kDa, and 150 kDa (Figure 2A). On the other hand, the 48.3 kDa protein band was found to be exclusively expressed in the planktonic fraction. Planktonic fraction demonstrated significantly ($p<0.05$) higher intensity of seven protein bands (33.7 kDa; 41.9 kDa, 58.5 kDa, 75 kDa, 100 kDa, 128.8 kDa, and 150 kDa) than biofilm fraction (Figure 2B).

Identified *C. pseudotuberculosis* proteins

A total of 854 and 387 proteins were successfully identified in planktonic and biofilm fractions, respectively (Figure 3). Of these, 589 proteins (60.35%) and 122 proteins (12.5%) were exclusively expressed in the planktonic and biofilm fractions, respectively. Meanwhile, 265 proteins (27.15%) were detected at both stages. It should be noted that the differentially expressed proteins herein represent the proteins that were present only in the planktonic or biofilm fraction. The basis of this consideration is that the *C. pseudotuberculosis* clinical isolate tends to form heterogeneous biofilm on the surface (Figure 1). Therefore, the subtractive approach is more suitable for the comparative proteomic analysis of biofilm (Yahya *et al*., 2017). A total of 711 proteins were found to be differentially expressed in *C. pseudotuberculosis* biofilm as compared to its planktonic counterpart. Ninety-four (13.22%) of them were found to be hypothetical proteins. The majority of differentially expressed *C. pseudotuberculosis* proteins were found to be linked to transcription and translation (32%), and the cytoplasmic compartment (73%) (Figure 4).

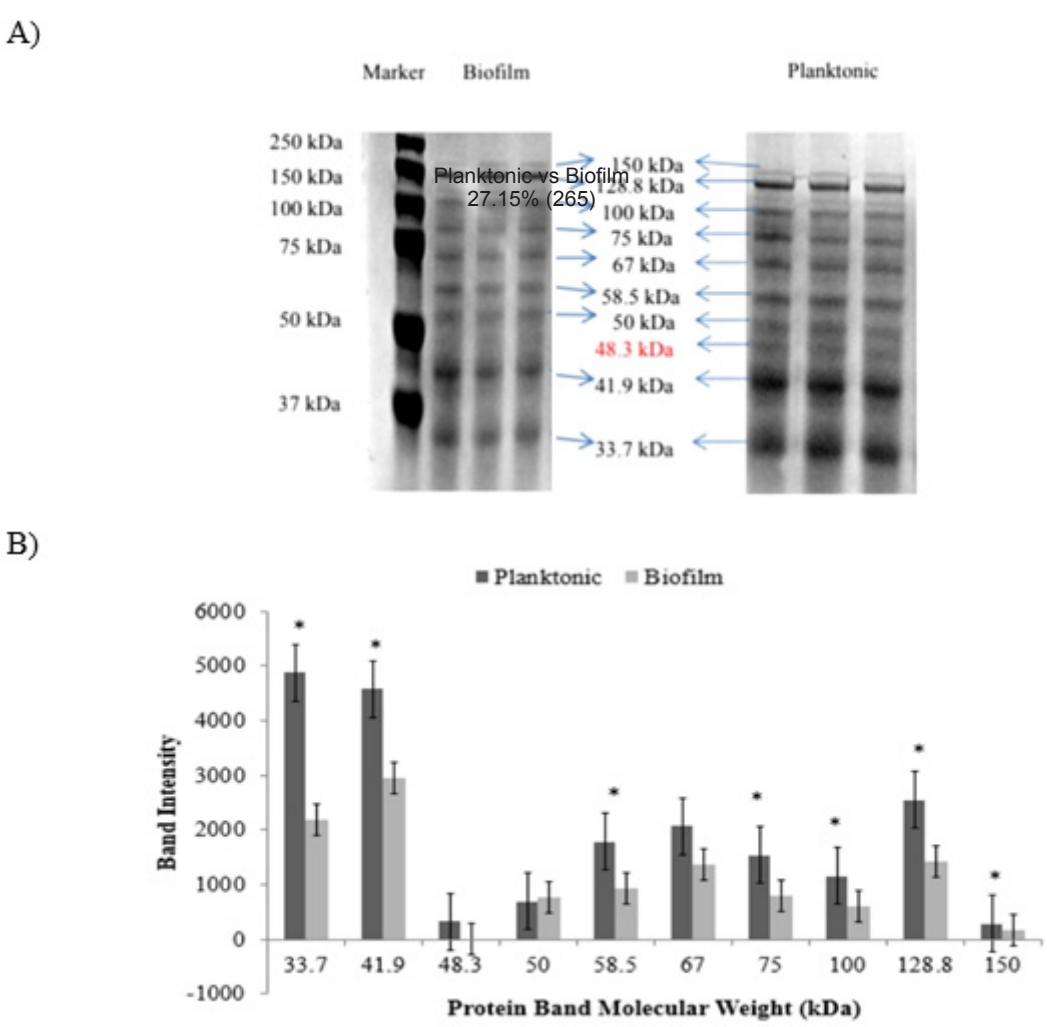

Fig. 2. Proteome profiles of *C. pseudotuberculosis*. A: Polyacrylamide gel stained with G250 Coomassie-Blue; B: Intensity of *C. pseudotuberculosis* protein bands in biofilm and planktonic fractions. Each bar represents the mean ± standard deviation. Significant differences (p<0.05) when compared between the two groups are shown by *.

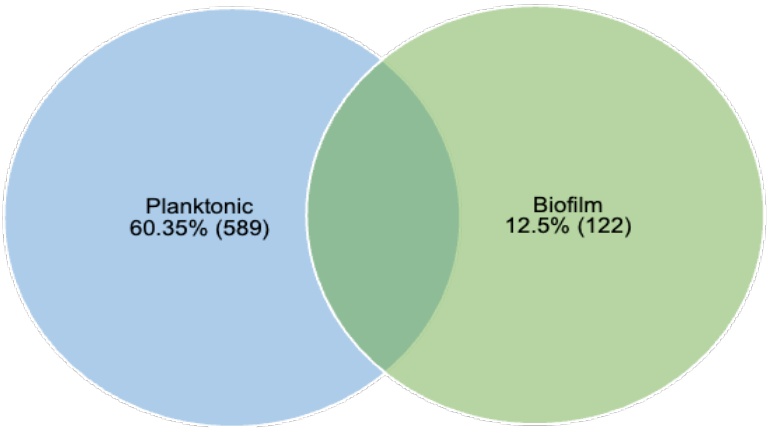

Fig. 3. Venn diagram for identified *C. pseudotuberculosis* proteins in the planktonic and biofilm fractions.

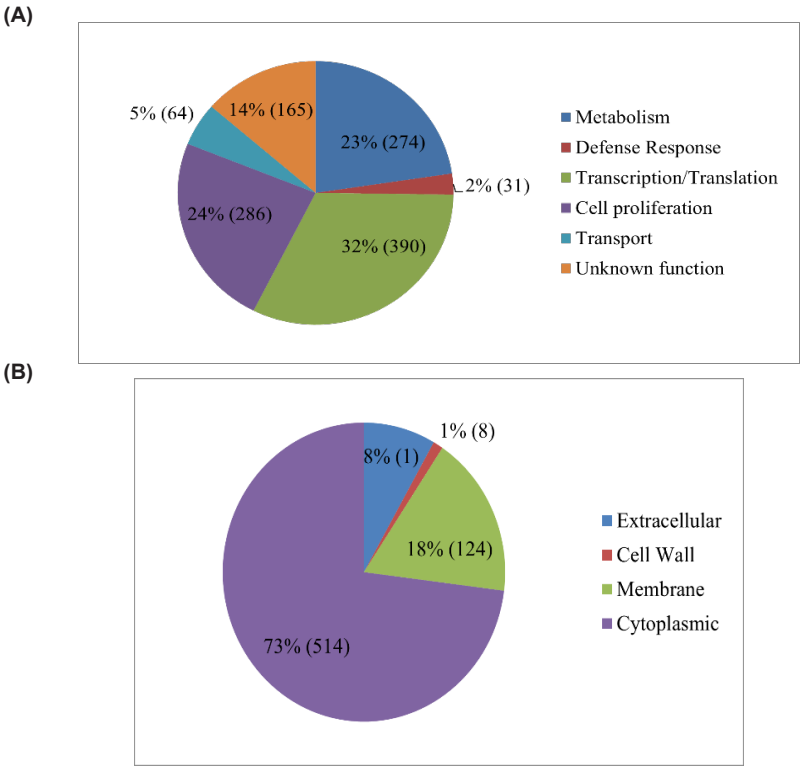

Fig. 4. Classification of differentially expressed proteins of *C. pseudotuberculosis* based on the SwissProt/TrEMBL database. (A) functional categories; (B) subcellular localizations.

Validation of proteomic expression by phosphoprotein assay

In this study, the proteomic data were validated using a phosphoprotein assay as previously reported (Yahya *et al*., 2017). A total of 23 phosphoproteins in *C. pseudotuberculosis* biofilm were identified by LC-MS/MS (Table 1). The presence of those phosphoproteins in *C. pseudotuberculosis* biofilm was validated by ProQ diamond staining, whereby two phosphoprotein bands, 33.7 kDa and 150 kDa, were detected (Figure 5).

Functional linkages between differentially expressed *C. pseudotuberculosis* proteins.

A total of 3868 functional interactions were produced among the differentially expressed *C. pseudotuberculosis* proteins, and they were classified into four clusters (Figure 6). Fifty-seven *C. pseudotuberculosis* proteins were considered as hub proteins as they showed more than 10 functional interactions in the network, including Phosphotransferase system II Component (24 interactions), Glycine hydroxy methyltransferase (25 interactions), Large subunit ribosomal protein L3 (26 interactions), Translation initiation factor IF-2 (29 interactions), multifunctional oxoglutarate decarboxylase (30 interactions) and DNA-dependent RNA polymerase (30 interactions). All the data from the network enrichment analysis were significant (*p-value*<0.05). A total of 123 differentially expressed *C. pseudotuberculosis* proteins were found to be associated with secondary metabolite biosynthesis.

Table 1. Phosphoproteins identified in *C. pseudotuberculosis* biofilm

m/z	Phosphoresidue	Score	Phosphopeptides/ Identified proteins
197.1284,311.2078, 507.3289	Ser-115	186	KL**S**VPCSDSK/ Chaperonin GroEL
283.0326,839.3369, 1080.4973	Ser-70, Ther-86	120	D**S**VGAVVMGPYADLQEG**T**KVK/ F0F1 ATP synthase subunit alpha
284.1605,848.4315, 1124.6245,1239.6514	Ther-84	96	S**T**LGRIMNVLGDPIDMK/ F0F1 ATP synthase subunit beta
563.2936, 773.4304	Ser-1296, Ther-1301/Ser-143	94	Q**S**KIPA**T**FSR/VLYFE**S**YVVIETGMTNL EKR/ DNA-directed RNA polymerase subunit beta
539.1861	Ser-273	72	GNVSGPDV**S**R/ ATP-dependent Clp protease ATP-binding subunit clpX
226.1298,227.1139, 244.1404,392.2054, 488.2099,523.2455, 783.4036,784.3876, 916.4411	Ser-176,180	65	YLDLI**S**NDE**S**R/ Lysyl-tRNA synthetase
1.2294,484.2716, 725.4143,838.4781, 909.5354,1209.6626	Ther-17	64	KTAIALAVALAGFA**T**VAQAAPK/ Histidine--tRNA ligase
298.1397,1009.5677	Ther-340,341,Ser-349	58	DV**TT**GDTLCVE**S**APIILER/ Elongation factor Tu
183.1128	Ther-194/ Ser-562, Ther-563	58	A**T**FNSEEK/I**S**TVPEAVEMQ**S**R/ Multifunctional oxoglutarate decarboxylase/ Oxoglutarate dehydrogenase thiamine pyrophosphate-binding subunit/ Dihydrolipoyllysine-residue succinyltransferase subunit
454.266, 793.5182	Ser-759, Ther-765	51	SLAI**S**LILQD**T**NR/ Phenylalanine--tRNA ligase subunit beta
213.131, 269.1969	Ther-26, Ser-28	51	VI**T**F**S**TGRLAR/ Polyribonucleotide nucleotidyltransferase
684.4039	Ser- 236,239, Ther-244	50	VPV**S**NV**S**VVDL**T**VR/ Type I glyceraldehyde-3- phosphate dehydrogenase
639.2498	Ther-190	47	IIAGTA**T**R/ methionyl-tRNA formyltransferase
389.2547,502.3388, 617.4021,732.429, 789.4505,876.4825	Ser-154/Ther-5	45	GE**S**YK/PII**T**LPDGSQR/ threonine--tRNA ligase
441.1995,484.2179, 582.2283,786.3182, 882.3757,994.4758	Ser-251	44	TIIGFG**S**PNK/transketolase
488.1541,829.3492	Ser-434	43	TLDLLY**S**R/trigger factor

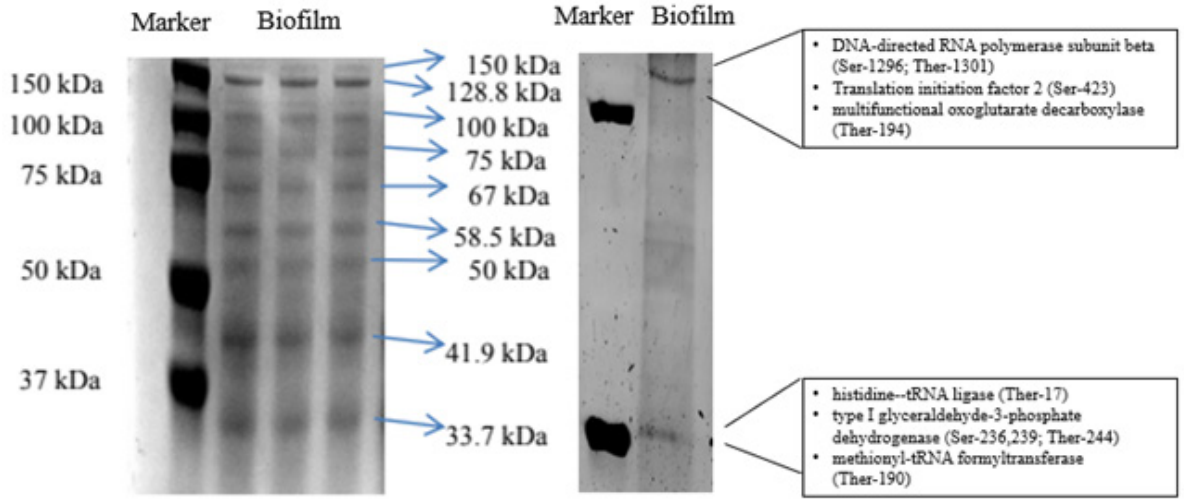

Fig. 5. Protein profiles of *C. pseudotuberculosis* biofilm stained with G250 Coomassie-Blue (Left) and ProQ Diamond staining (right). Representative phosphoproteins for respective protein bands are shown in the boxes.

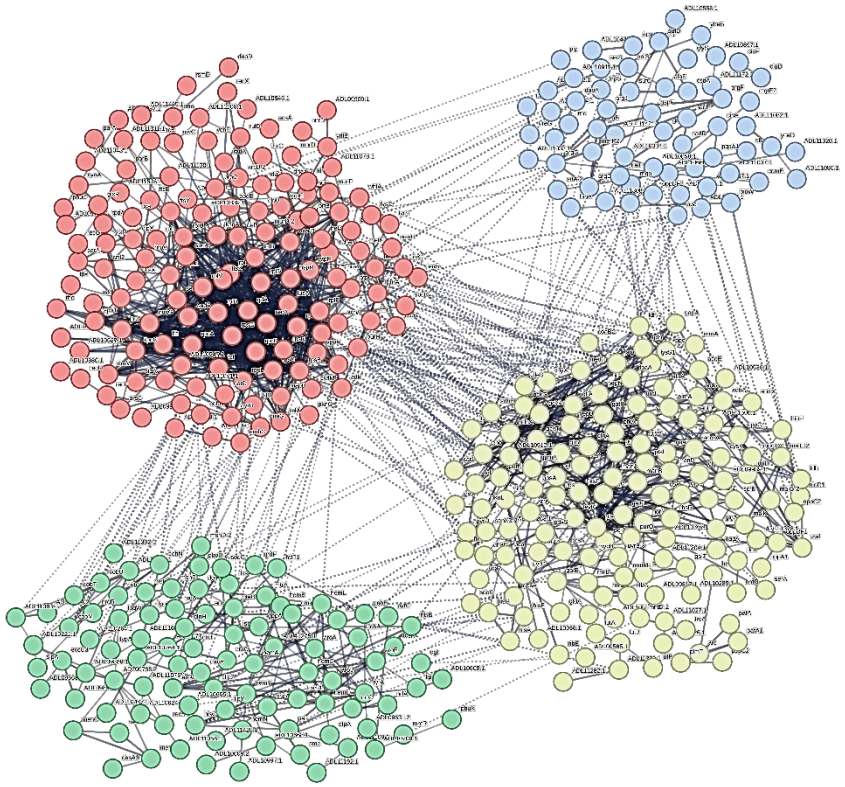

Fig. 6. Non-overlapping clusters of differentially expressed proteins in *C. pseudotuberculosis* during biofilm formation. The analysis was performed using the k-means clustering algorithm in the STRING database v.11.0. Cluster 1 (red): Cellular macromolecule metabolism, nucleic acid binding, gene expression, and protein transport; Cluster 2 (yellow): Small molecule metabolism, metabolic pathways; Cluster 3 (green): Unknown; Cluster 4 (blue): Unknown.

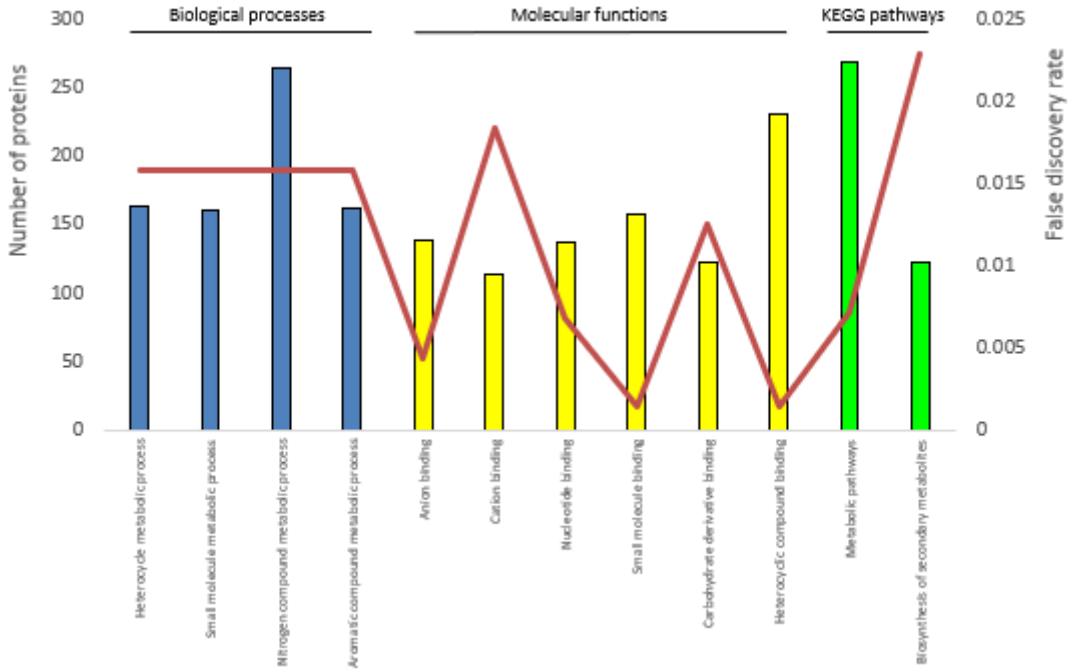

Fig. 7. Functional enrichment of *C. pseudotuberculosis* protein-protein interaction network.

Hypothetical protein Cp106_2054

Hypothetical proteins with more than 1000 residues are often prioritized for *in silico* analysis due to their potential functional complexity and higher likelihood of containing multiple domains or motifs that may play critical roles in biological processes (Schütze *et al*., 2022). Their large size suggests they could encode structurally intricate proteins with catalytic, regulatory, or scaffolding functions, making them prime candidates for uncovering novel mechanisms. Hypothetical protein Cp106_2054 was further analyzed for its functional characteristics, as it has more than 1000 amino acids. It was predicted to contain 15 transmembrane helices, the MviN domain, which plays a role in peptidoglycan biosynthesis, and several post-translational modification sites, such as casein kinase II phosphorylation and cGMP-dependent protein kinase phosphorylation site (Figure 8). It also showed an instability index of 35.01, classifying the protein as stable. Template 6cc4.1.A (a soluble cytochrome from *Escherichia coli*) was used to construct the 3D model of this hypothetical protein. The sequence similarity between the target and template was found to be 22.83%. The 3D model showed Ramachandran-favored area of 93.18%. Hypothetical protein Cp106_2054 was also predicted to have functional linkages with other proteins involved in the peptidoglycan metabolic pathway (p<0.05).

DISCUSSION

C. pseudotuberculosis is the etiologic agent of CLA. While many reports have shown that this disease primarily affects goats and sheep, it also infects humans (Dopud *et al*. 2025). This disease is prevalent in commercial regions of small ruminant-based products (Soares *et al*., 2013). In the last few years, the study of *C. pseudotuberculosis* biofilm has dramatically increased (Santos *et al*., 2018; Yaacob *et al*., 2021; Santos *et al*., 2024; Saddiqi & Kadir, 2024). By considering the fact that the biofilm is key to microbial pathogenesis, our current focus is to elucidate the proteomic expression during the development of *C. pseudotuberculosis* biofilm. The present study bridges gaps in *C. pseudotuberculosis* biofilm biology by combining electrophoretic profiling, protein-protein interactions (PPI) networks, and functional annotation. The methodological synergy, from wet-lab protein separation to *in silico* network modelling, sets a precedent for studying other neglected pathogens.

The morphology of *C. pseudotuberculosis* biofilm has previously been characterized using FESEM (Yaacob *et al*., 2021a; Rashid *et al*., 2022). They demonstrated extracellular matrix, a heterogeneous 3D structure, and pores in *C. pseudotuberculosis* biofilm. Therefore, the present study used the same experimental approach to verify the biofilm formation before proteomic analysis.

The present study revealed that nine protein bands (33.7–150 kDa) were shared between planktonic and biofilm fractions of *C. pseudotuberculosis*, suggesting conserved molecular machinery across both lifestyles. Notably, the detection of 38 kDa and 58 kDa proteins in the biofilm fraction contrasts with Braithwaite *et al*. (1993), who identified these bands only in whole-cell lysates. This discrepancy highlights a differential expression pattern during biofilm formation, implying these proteins may play stage-specific roles in adhesion, matrix assembly, or stress adaptation. The presence of a 100 kDa band, previously reported in secreted proteins (dos Santos *et al*., 2022), further underscores the biofilm's active secretion system, potentially contributing to virulence or nutrient acquisition. These findings advance the understanding of *C. pseudotuberculosis* pathogenicity by linking specific proteins to biofilm-specific adaptations.

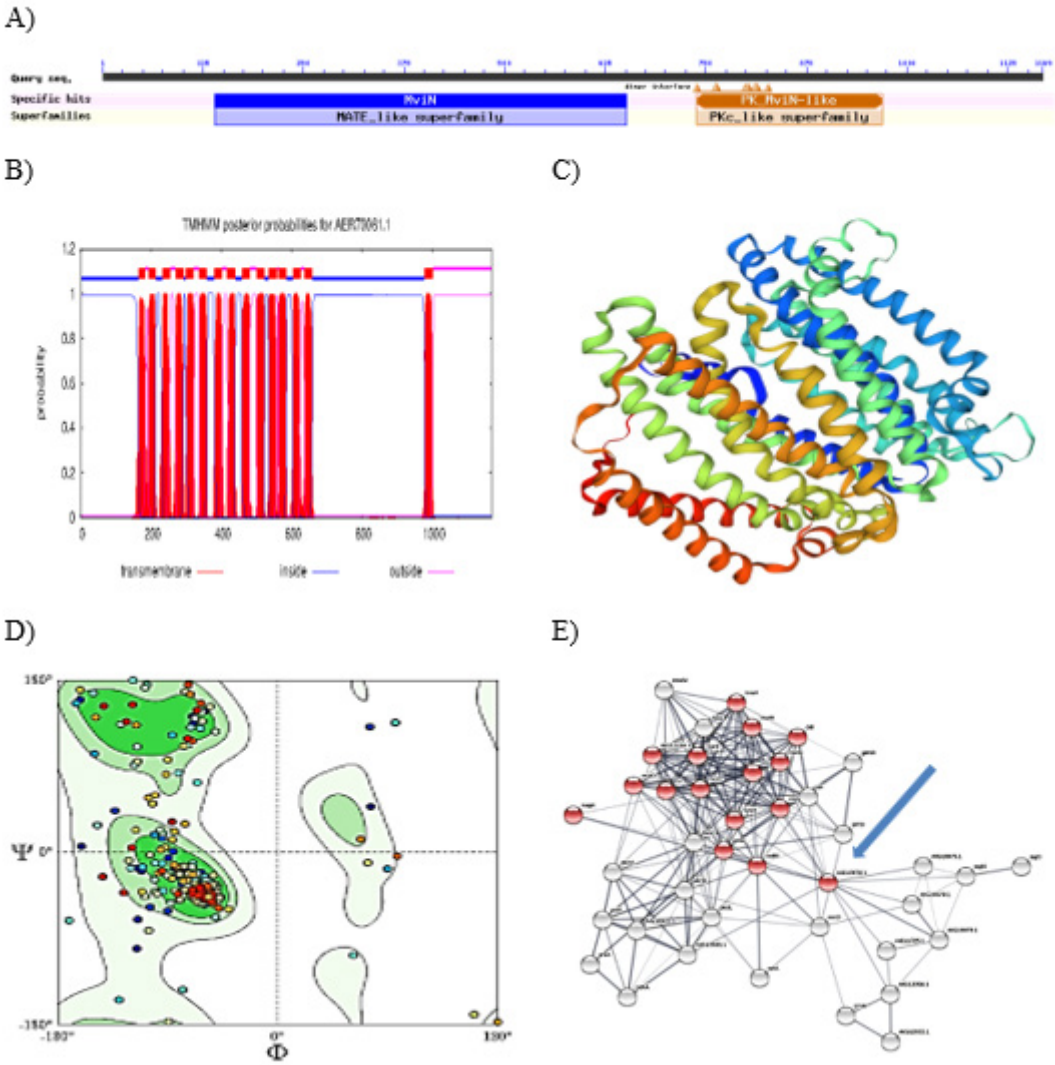

Fig. 8. Functional characteristics of hypothetical protein Cp106_2054. A: MviN and PK_MviN-like domains; B: transmembrane domain; C: 3D model based on homology modelling; D: Ramachandran plot; E: proteins associated with peptidoglycan metabolism in protein-protein interaction network are marked in red, while the blue arrow indicates hypothetical protein Cp106_2054.

The present study successfully identified a total of 976 *C. pseudotuberculosis* proteins. Subtractive analysis revealed 711 proteins that were differentially expressed between biofilm and planktonic fractions. The majority of identified proteins were related to transcription/translation and the cytoplasmic compartment. Several lines of proteomic work have used the subtractive approach to analyze complex and heterogeneous proteome samples to solve the potential problem of a large range of protein expression levels (Schirmer *et al*., 2003; Yahya *et al*., 2017). Meanwhile, De Sá *et al*. (2021) have identified 40 proteins that were differentially expressed between biofilm producers and non-biofilm producers of *C. pseudotuberculosis*. Differential proteomic expression observed in the present study also corroborates the fact that the biofilm state exhibits a different proteome expression profile as compared to that of the planktonic state (Yaacob *et al*., 2021b). Proteins associated with carbohydrate metabolism (phosphoglyceromutase and pyruvate dehydrogenase) were noticed to be differentially expressed in *C. pseudotuberculosis* biofilm. They probably play roles in the oxygen-limited environment and the synthesis of core biofilm matrix (Suryaletha *et al*., 2019). Furthermore, proteins associated with amino acid metabolism (Cysteine synthase A and Glutamine synthetase II) were also found to be differentially expressed in *C. pseudotuberculosis* biofilm. They may participate in the synthesis of the extracellular matrix of robust biofilm (Suryaletha *et al*., 2019).

The PPI network analysis identified 57 highly connected hub proteins, revealing the biofilm's reliance on multifunctional coordinators to integrate metabolic and structural pathways. This aligns with Huang *et al*. (2019), who emphasized the centrality of hubs in biofilm resilience. Crucially, Folador *et al*. (2016) demonstrated that hub proteins in *C. pseudotuberculosis* are essential for survival, suggesting their disruption could affect biofilm integrity. The conservation of such hubs in other biofilm-forming pathogens (Yahya *et al*., 2017; Isa *et al*., 2022) implies broad applicability, positioning these proteins as cross-species therapeutic candidates for CLA and related chronic infections.

Functional enrichment analysis has been widely used to link the properties of protein sequences with relevant functional categories. Most functional enrichment tools are web-based and focused on specific contexts. Functional enrichment analysis using the STRING database demonstrated in the present study successfully characterized the *C. pseudotuberculosis* proteome.

It allows identification of various biological processes and pathways involved in the formation of *C. pseudotuberculosis* biofilm by quantitative measurement using a common and well-known statistical method, namely Fisher's exact test (Szklarczyk *et al*., 2017). We found that biosynthesis of amino acids and biosynthesis of secondary metabolites (Figure 8) were significantly enriched (p<0.005) in the network of differentially expressed proteins. This result agrees with Santos *et al*. (2018) reporting similar significant pathways in the proteome dataset of *C. pseudotuberculosis* collected from the NCBI GenPept database. The use of bioinformatics tools is vital to advance global functional analysis of the *C. pseudotuberculosis* genome (Da Silva *et al*., 2021)

GalT is a protein responsible for breaking down galactose via the Leloir pathway, which plays a role in exopolysaccharide biosynthesis. The catalytic activity of this protein is dependent on metallic trace elements such as zinc and iron. In the present study, galactose-1-phosphate uridyltransferase was found to be expressed in the planktonic fraction but was not expressed in the biofilm fraction. This result corroborates De Sá *et al*. (2021), demonstrating differential expression of GalT in *C. pseudotuberculosis* biofilm (CAPJ4 strain). The GalT family member is required for the regulation of biofilm formation through purine biosynthesis (Monds *et al*., 2010). It is possible that the expression of this protein family is required during the early biofilm stage, but is not required when *C. pseudotuberculosis* has reached the mature and heterogeneous biofilm stage.

clpB plays a role in ATP binding, protein folding, and stress response, which promotes the survival of microbial cells. The present study showed that ATP-dependent chaperone clpB was expressed in the biofilm fraction but was not expressed in the planktonic fraction. According to Petrova and Sauer (2012), clpB is required for the function of chemotaxis protein BdlA in the dispersion of *Pseudomonas aeruginosa* biofilm. This has led us to assume that the clpB expression may also be required for dispersion of *C. pseudotuberculosis* biofilm.

GrpE is a cochaperone that promotes dissociation of ADP from the nucleotide-binding cleft of DnaK. GrpE plays prominent roles in protein folding. The present study showed that nucleotide exchange factor GrpE was expressed in the planktonic fraction but was not expressed in the biofilm fraction. Changes in the expression of this protein during biofilm formation are not well investigated; however, Gomide *et al*. (2018) have demonstrated differential expression of the *grpE* gene in *C. pseudotuberculosis* following heat shock stress. GrpE is likely required during the transition from the planktonic stage to the biofilm stage of *C. pseudotuberculosis*.

Our *in silico* data have predicted that hypothetical protein Cp106_2054 may function as a transmembrane protein that participates in peptidoglycan metabolism. This suggestion is in line with the fact that transmembrane protein complexes play important roles in peptidoglycan metabolism (Formstone *et al*., 2008). Differential expression of this hypothetical protein during the biofilm formation by *C. pseudotuberculosis* is consistent with Li *et al*. (2014), demonstrating differential expression of proteins involved in peptidoglycan biosynthesis during the formation of *Actinobacillus pleuropneumoniae* biofilm. In the present study, we used the re-centering function available in the STRING database to analyze the network of differentially expressed *C. pseudotuberculosis* proteins in detail, thereby allowing identification of the peptidoglycan biosynthetic pathway. That database function enables users to identify what types of proteins exist around the protein of interest in the protein-protein interaction network, which is useful to unravel new protein functions that are hidden in large and complex biological networks (Praneenararat *et al*., 2012). Our findings highlight the importance of peptidoglycan metabolism in *C. pseudotuberculosis* biofilm formation and suggest potential therapeutic approaches, such as targeting PG synthesis.

CONCLUSION

Differential proteome expression in *C. pseudotuberculosis* biofilms reveals key functional hub proteins such as phosphotransferase system II Component, glycine hydroxy methyltransferase, large subunit ribosomal protein L3, translation initiation factor IF-2, multifunctional oxoglutarate decarboxylase, and DNA-dependent RNA polymerase. They may modulate adaptive responses to environmental stressors, thereby promoting biofilm formation. The results of this study could contribute to improved strategies for controlling CLA disease.

ACKNOWLEDGEMENTS

This research was funded by the Pembiayaan Yuran Penerbitan Artikel (PYPA), Universiti Teknologi MARA.

ETHICAL STATEMENT

Not applicable.

CONFLICT OF INTEREST

The authors declare no conflict of interest.

REFERENCES

Braithwaite, C.E., Smith, E.E., Songer, J.G. & Reine, A.H. 1993. Characterization of detergent-soluble proteins of *Corynebacterium pseudotuberculosis*. Veterinary Microbiology, 38(1-2): 59-70. https://doi.org/10.1016/0378-1135(93)90075-I

Cho, J.A., Jeon, S., Kwon, Y., Roh, Y.J., Lee, C.H. & Kim, S.J. 2024. Comparative proteomics analysis of biofilms and planktonic cells of *Enterococcus faecalis* and *Staphylococcus lugdunensis* with contrasting biofilm-forming ability. PLoS One, 19(5): e0298283. https://doi.org/10.1371/journal.pone.0298283

Da Silva, W.M., Seyffert, N., Silva, A. & Azevedo, V. 2021. A journey through the *Corynebacterium pseudotuberculosis* proteome promotes insights into its functional genome. PeerJ, 9: e12456. https://doi.org/10.7717/peerj.12456

De Sá, M.C.A., Da Silva, W.M., Rodrigues, C.C.S., Rezende, C.P., Marchioro, S.B., Rocha, J.T.R., de Sousa, T.J., Oliveira, H.P., Costa, M.M., Figueiredo, H.C.P., Portela, R.D., Castro, T.L.P., Azevedo, V., Seyffert, N. & Meyer, R. 2021. Comparative proteomic analyses between biofilm-forming and non-biofilm-forming strains of *Corynebacterium pseudotuberculosis*

isolated from goats. Frontiers in Veterinary Science, 8: 614011. https://doi.org/10.3389/fvets.2021.614011

Dopuđ, M., Reil, I., Zdelar-Tuk, M., Špičić, S. & Duvnjak, S. 2025. *Caseous lymphadenitis* in sheep and goats-"Cheese glands". Veterinarska Stanica, 56(3): 303-316. https://doi.org/10.46419/vs.56.3.8

dos Santos, R.M., Cerqueira, S.M.A., Andrade, C.L.B., Müller, G.S., de Menezes Santos, V.C., de Araújo, H.R., Queiroz, S., Conceicao, R.R., Oliveira, L.G.F., Ribeiro, M.B., Marchioro, S., de Moura-costa, L.F., de Sousa, F.S.C., de Sá, M.D.C.A., Filho, J.T.R.R., Trindade, S.C., Netto, E.M., Meyer, R. & Freire, S.M. 2022. Human seroreactivity to secreted molecules of *Corynebacterium pseudotuberculosis*. Advances in Microbiology, 12(3): 150-158. https://doi.org/10.4236/aim.2022.123012

Dsouza, F.P., Dinesh, S. & Sharma, S. 2024. Understanding the intricacies of microbial biofilm formation and its endurance in chronic infections: A key to advancing biofilm-targeted therapeutic strategies. Archives of Microbiology, 206(2): 85. https://doi.org/10.1007/s00203-023-03802-7

Eberle, R.J., Kawai, L.A., de Moraes, F.R., Tasic, L., Arni, R.K. & Coronaso, M.A. 2018. Biochemical and biophysical characterization of a mycoredoxin protein glutaredoxin A1 from *Corynebacterium pseudotuberculosis*. International Journal of Biological Macromolecules, 107(Part B): 1999-2007. https://doi.org/10.1016/j.ijbiomac.2017.10.063

Folador, E.L., de Carvalho, P.V.S.D., Silva, W.M., Ferreira, R.S., Silva, A., Gromiha, M., Ghosh, P., Barth, D., Azevedo, V. & Röttger, R. 2016. *In silico* identification of essential proteins in *Corynebacterium pseudotuberculosis* based on protein-protein interaction networks. BMC Systems Biology, 10: 103. https://doi.org/10.1186/s12918-016-0346-4

Formstone, A., Carballido-López, R., Noirot, P., Errington, J. & Scheffers, D.J. 2008. Localization and interactions of teichoic acid synthetic enzymes in *Bacillus subtilis*. Journal of Bacteriology, 190(5): 1812-1821. https://doi.org/10.1128/JB.01394-07

Gomide, A.C.P., de Sá, P.G., Cavalcante, A.L.Q., de Jesus Sousa, T., Gomes, L.G.R., Ramos, R.T.J., Azevedo, V., Silva, A. & Folador, A.R.C. 2017. Heat shock stress: profile of differential expression in *Corynebacterium pseudotuberculosis* biovar equi. Gene, 645: 124-130. https://doi.org/10.1016/j.gene.2017.12.015

Gomide, A.C.P., Ibraim, I.C., Alves, J.T.C., de Sá, P.G., de Oliveira Silva, Y.R., Santana, M.P., Silva, W.M., Folador, E.L., Mariano, D.C.B., de Paula Castro, T.L., Barbosa, S., Dorella, F.A., Carvalho, A.F., Pereira, F.L., Leal, C.A.G., Figueiredo, H.C.P., Azevedo, V., Silva, A. & Folador, A.R.C. 2018. Transcriptome analysis of *Corynebacterium pseudotuberculosis* biovar equi in two conditions of the environmental stress. Gene, 677: 349-360. https://doi.org/10.1016/j.gene.2018.08.028

Huang, Z., Wang, Y.H., Zhu, H.Z., Andrianova, E.P., Jiang, C.Y., Li, D., Ma, L., Feng, J., Liu, Z.P., Xiang, H., Zhulin, I.B. & Liu, S.J. 2019. Cross talk between chemosensory pathways that modulate chemotaxis and biofilm formation. mBio, 10(1): e02876-18. https://doi.org/10.1128/mBio.02876-18

Isa, S.F.M., Hamida, U.M.A. & Yahya, M.F.Z.R. 2022. Treatment with the combined antimicrobials triggers proteomic changes in *Pseudomonas aeruginosa* - *Candida albicans* polyspecies biofilms. ScienceAsia, 48(2): 215-222. https://doi.org/10.2306/scienceasia1513-1874.2022.020

Li, L., Zhu, J., Yang, K., Xu, Z., Liu, Z. & Zhou, R. 2014. Changes in gene expression of *Actinobacillus pleuropneumoniae* in response to anaerobic stress reveal induction of central metabolism and biofilm formation. Journal of Microbiology, 52(6): 473-481. https://doi.org/10.1007/s12275-014-3456-y

Monds, R.D., Newell, P.D., Wagner, J.C., Schwartzman, J.A., Lu, W., Rabinowitz, J.D. & O'Toole, G.A. 2010. Di-adenosine tetraphosphate (Ap4A) metabolism impacts biofilm formation by *Pseudomonas fluorescens* via modulation of c-di-GMP-dependent pathways. Journal of Bacteriology, 192(12): 3011-3023. https://doi.org/10.1128/JB.01571-09

Othman, N.A. & Yahya, M.F.Z.R. 2019. In silico analysis of essential and non-homologous proteins in *Salmonella typhimurium* biofilm. Journal of Physics: Conference Series, 1349(1): 012133. https://doi.org/10.1088/1742-6596/1349/1/012133

Percival, S.L., Suleman, L., Vuotto, C. & Donelli, G. 2015. Healthcare-associated infections, medical devices and biofilms: Risk, tolerance and control. Journal of Medical Microbiology, 64: 323-334. https://doi.org/10.1099/jmm.0.000032

Petrova, O.E. & Sauer, K. 2012. Dispersion by Pseudomonas aeruginosa requires an unusual posttranslational modification of BdlA. Proceedings of the National Academy of Sciences, 109(41): 16690-16695. https://doi.org/10.1073/pnas.1207832109

Praneenararat, T., Takagi, T. & Iwasaki, W. 2012. Integration of interactive, multi-scale network navigation approach with Cytoscape for functional genomics in the big data era. BMC Genomics, 13: 1-10. https://doi.org/10.1186/1471-2164-13-S7-S24

Rashid, S.A.A., Yaacob, M.F., Aazmi, M.S., Jesse, F.F.A. & Yahya, M.F.Z.R. 2022. Inhibition of Corynebacterium pseudotuberculosis biofilm by DNA and protein synthesis inhibitors. Journal of Sustainability Science and Management, 17(4): 49-56. https://doi.org/10.46754/jssm.2022.4.004

Saddiqi, M. & Kadir, A.A. 2024. Antibacterial activity of free and liposome-encapsulated Tylosin against planktonic and biofilm forms of *Corynebacterium pseudotuberculosis* isolated from goats. Acta Veterinaria Eurasia, 50(2).

Santos, E.M.S., Almeida, A.C., Santos, H.O., Cangussu, A.S.R., Almeida, D.A. & Costa, K.S. 2018. Leader gene of *Corynebacterium pseudotuberculosis* may be useful in vaccines against caseous lymphadenitis of goats: A bioinformatics approach. Journal of Veterinary Medical Science, 80(8): 1317-1324. https://doi.org/10.1292/jvms.16-0581

Santos, L.M., Rodrigues, D.M., Alves, B.V.B., Kalil, M.A., Azevedo, V., Barh, D. & Portela, R.W. 2024. Activity of biogenic silver nanoparticles in planktonic and biofilm-associated *Corynebacterium pseudotuberculosis*. PeerJ, 12: e16751. https://doi.org/10.7717/peerj.16751

Schirmer, E.C., Florens, L., Guan, T., Yates, J.R. & Gerace, L. 2003. Nuclear membrane proteins with potential disease links found by subtractive proteomics. Science, 301(5638): 1380-1382. https://doi.org/10.1126/science.1088176

Schütze, K., Heinzinger, M., Steinegger, M. & Rost, B. 2022. Nearest neighbor search on embeddings rapidly identifies distant protein relations. Frontiers in Bioinformatics, 2: 1033775. https://doi.org/10.3389/fbinf.2022.1033775

Soares, S.C., Trost, E., Ramos, R.T.J., Carneiro, A.R., Santos, A.R., Pinto, A.C., Barbosa, E., Aburjaile, F., Ali, A., Diniz, C.A.A., Hassan, S.S., Fiaux, K., Guimarães, L.C., Bakhtiar, S.M., Pereira, U., Almeida, S.S., Abreu, V.A.C., Rocha, F.S., Dorella, F.A., Miyoshi, A., Silva, A., Azevedo, V. & Tauch, A. 2013. Genome sequence of *Corynebacterium pseudotuberculosis* biovar equi strain 258 and prediction of antigenic targets to improve biotechnological vaccine production. Journal of Biotechnology, 167(2): 135-141. https://doi.org/10.1016/j.jbiotec.2012.11.003

Stoodley, P., Sauer, K., Davies, D.G. & Costerton, J.W. 2002. Biofilms as complex differentiated communities. Annual Review of Microbiology, 56: 187-209. https://doi.org/10.1146/annurev.micro.56.012302.160705

Sung, K., Park, M., Chon, J., Kweon, O., Paredes, A. & Khan, S.A. 2024. Chicken juice enhances *C. jejuni* NCTC 11168 biofilm formation with distinct morphological features and altered protein expression. Foods, 13(12): 1828. https://doi.org/10.3390/foods13121828

Sung, K., Park, M., Kweon, O., Paredes, A., Savenka, A. & Khan, S.A. 2025. Proteomic insights into dual-species biofilm formation of *E. coli* and *E. faecalis* on urinary catheters. Scientific Reports, 15(1): 3739. https://doi.org/10.1038/s41598-024-81953-3

Suryaletha, K., Narendrakumar, L., John, J., Radhakrishnan, M.P., George, S. & Thomas, S. 2019. Decoding the proteomic changes involved in the biofilm formation of Enterococcus faecalis SK460 to elucidate potential biofilm determinants. BMC Microbiology, 19: 146. https://doi.org/10.1186/s12866-019-1527-2

Szklarczyk, D., Morris, J.H., Cook, H., Kuhn, M., Wyder, S., Simonovic, M., Santos, A., Doncheva, N.T., Roth, A., Bork, P., Jensen, L.J. & von Mering, C. 2017. The STRING database in 2017: Quality-controlled protein-protein interaction networks, made broadly accessible. Nucleic Acids Research, 45(D1): D362-D368. https://doi.org/10.1093/nar/gkw937

Yaacob, M.F., Johari, N.A., Kamaruzzaman, A.N.A. & Yahya, M.F.Z.R. 2021b. Mass spectrometry-based proteomic investigation of heterogeneous biofilms: A review. Scientific Research Journal, 18(2): 67-87. https://doi.org/10.24191/srj.v18i2.11718

Yaacob, M.F., Murata, A., Nor, N.H.M., Jesse, F.F.A. & Yahya, M.F.Z.R. 2021a. Biochemical composition, morphology and antimicrobial susceptibility pattern of Corynebacterium pseudotuberculosis biofilm. Journal of King Saud University - Science, 33(1): 101225. https://doi.org/10.1016/j.jksus.2020.10.022

Yahya, M.F.Z.R., Alias, Z. & Karsani, S.A. 2017. Subtractive protein profiling of *Salmonella typhimurium* biofilm treated with DMSO. The Protein Journal, 36: 286-298. https://doi.org/10.1007/s10930-017-9719-9

Zawawi, W.M.A.W.M., Ibrahim, M.S.A., Rahmad, N., Hamid, U.M.A. & Yahya, M.F.Z.R. 2020. Proteomic analysis of Pseudomonas aeruginosa biofilm treated with *Chromolaena odorata* extracts. Malaysian Journal of Microbiology, 16(2): 124-133. https://doi.org/10.21161/mjm.190512